ORIGINAL ARTICLE

A comprehensive characterization of non-edible lignocellulosic biomass to elucidate their biofuel production potential

Abhisek Sahoo[1] · Sachin Kumar[1,2] (ID) · Kaustubha Mohanty[3]

Abstract

It is very requisite to demonstrate the characterization of lignocellulosic biomass for converting into renewable fuels and valuable chemicals. In this work, the physicochemical and thermochemical characterization of some non-edible oil seeds such as Putranjiva (*Putranjiva roxburghii*), Amaltas (*Cassia fistula*), and Siris (*Albizia lebbeck*) were carried out by extractive analysis via Soxhlet solvent extraction, compositional analysis, proximate analysis, elemental (CHNSO) analysis, heating value, bulk density, crystallinity index via XRD, functional groups via FTIR, mineral content via EDX, slagging and fouling indices via XRF, and degradation profile via TGA. It was noticed that all seeds consist of a maximum percentage of extractives such as Putranjiva 50.55%, Amaltas 18.22%, and Siris 22.8%. The results showed that these seeds have a higher cellulose content compared with hemicellulose and lignin. Further, it was confirmed from the Van Krevelen diagram, CHO index, as well as devolatilization index. Also, from the kinetic analysis, the activation energy (E_a) obtained of these seeds was in the order of PR > AL > CF. The chemical features and thermal degradation behaviour reaffirmed that these non-edible oilseeds have good energy potential for reproducibility of biofuel and green chemicals production.

Keywords Putranjiva roxburghii, Cassia fistula and Albizia lebbeck · Lignocellulosic biomass · Devolatilization index · FTIR · TGA

1 Introduction

The world energy demand increases rapidly due to the living standards improvement, urbanization, industrialization, and new technology developments. The global energy demand grows by 25% between 2017 and 2040 due to the rapid growth of the world population, which is expected to become 9.1 billion in 2040. The world energy outlook reported that energy demand would be more than doubles to 2040 in India [1]. In the year 2018, 34% oil, 27% coal, 24% natural gas, 7% hydro, 4% nuclear, and 4% renewable contributed to global energy consumption; 2% carbon emission grew up, and around 10% is the average growth of biofuels production [2]. The costs and requirements of fossil fuels are increasing with time. To reduce the amount of GHG emission and the scaling down of fossil fuel consumption, it is vital to discover alternative nonconventional sources of energy. The present energy sources are not abundant to fulfil our future demand. So, it has become a significant point of consideration for the researcher to focus on renewable energy sources such as sunlight, geothermal heat, waves, wind, tides, and biomass [3]. Due to adverse environmental impacts in terms of land reduction and contamination, the requirement of substantial agricultural lands, high water, and manure necessities, rivalry with food supplies, the utilization of first-generation biofuel feedstock generated several disputes with food versus fuel and afterward researchers looked for the second-generation of biofuel feedstocks. Now, it is time to focus on the alternative fuels

✉ Sachin Kumar
  sachin.kumar.01@cuj.ac.in

  Abhisek Sahoo
  sahooabhisek01@yahoo.com

  Kaustubha Mohanty
  kmohanty@iitg.ac.in

1 Department of Energy Engineering, Central University of Jharkhand (CUJ), Ranchi 835205, India

2 Centre of Excellence-Green and Efficient Energy Technology (CoE-GEET), Central University of Jharkhand, 835205 Ranchi, India

3 Department of Chemical Engineering, Indian Institute of Technology, Guwahati 721039, India

for substituting fossil fuels and mitigate the global warming and greenhouse gas effect. Lignocellulosic biomass is a plenteous and inexpensive source of renewable energy. Compared to other lignocellulosic biomass resources, few studies on the characteristics of non-edible oilseeds and their feasibility for the development of value-added products and biofuels have been carried out [4–7].

Putranjiva roxburghii (Putranjiva) is an evergreen tree. Its height is up to 12 m long. It has dark grey cortexes and overhanging offshoots. Fruits are rounded in shape, white in color, drupes, and velvety; seed usually stone pointed and very hard. Its fruits appear period is between January and March and flowering from March to April. The pharmacognosy of its fruits and leaves demonstrates a lot of saponins, glycosides, flavonoids, and triterpenes. The extracted oil from this seed is used for renewable fuel while blending up to 30–40% with diesel. It is distributed in various regions, including in Thailand, Nepal, Bangladesh, India, Myanmar, and Sri Lanka [8].

Cassia fistula (Amaltas) is a deciduous and medium-sized tree. It has compound leaves and greenish-grey cortexes. It is growing up to 24 m in height and 1.8 m in width, cultivated across India. Seed diameter is about 0.25 to 0.5 in. with a flattened, smooth, and teardrop in shape. Seeds are mildly poisonous, and it can cause diarrhea and vomiting when ingested. The tree is one of the most wide-spread in the Indian forest, usually taking place in deciduous forests, commonly across the Gangetic valley, particularly abundant in South India and Central India. It is grown along the roadside and in homesteads as an ornamental tree. It is widely spread in Asia, China, Brazil, West Indies, and South Africa [9].

Albizia lebbeck (Siris) is a fast-growing, versatile tree. Its fruit has a flat shaped, linear pod, and it is up to 30 cm long with many seeds. It also provides fuelwood. Its leaf indicates 16–26% crude protein and is an outstanding source of fodder. It is planted as an ornamental tree due to its pleasant appearance. It could be binding the soil and prevents soil erosion due to its root shapes. It is cultivated in homesteads, along roadsides, and irrigated plantations. It is widespread in dense deciduous forests across tropical and subtropical countries of Asia, Africa, Australia, Indonesia, Malaysia, Thailand, and China; and also the species are native to India, Myanmar, and the Andaman Island [10].

It is essential to mention that the availability of these non-edible oilseeds, which may be the foremost downside of this feedstock, has not yet reported in any literature. However, as per the India State of Forest Report (ISFR), 2017 total forest and tree cover is 8,02,088 km², which is 24.39% of the total geographical area of India, it can be claimed that India has an ample amount of seed to be used to generate alternative fuels or green chemicals from these seeds. Due to the ease of production, advantages of availability, and environmental benefits, biomass have attracted attention for renewable energy

sources. In the literature reported that for similar biomass, the handling and processing cost of these biomasses would be inexpensive [11]. Plant taxonomy of these non-edible oilseeds is presented in Table 1.

The comprehensive characterizations of these non-edible seeds have not been studied yet. In this present study, the physicochemical and thermochemical characterization were comprehensively investigated using a series of quantitative and qualitative analysis methods such as extractive analysis, compositional analysis, proximate analysis, elemental analysis, thermal analysis via TGA, functional groups analysis via FTIR, crystallinity index analysis via XRD, mineral content analysis via EDX, and higher heating value to demonstrate their feasibility of biofuel production. The residual composition of biomass was also determined via XRF analysis to gain a more in-depth insight into its potential impact during conversion processes. Furthermore, it is essential to know their physical, chemical, and thermal characteristics before using these oilseeds as a feedstock for pyrolysis or any thermochemical conversion process.

2 Materials and experimental methods

2.1 Sample collection and preparation

In this study, *Cassia fistula* (CF) and *Albizia lebbeck* (AL) seeds were collected from Coimbatore district, Tamilnadu, India. *Putranjiva roxburghii* (PR) seed was collected from Jaipur district, Rajasthan, India. The collected oilseeds were exposed to sunlight for 24–36 h and stored in an airtight plastic container. After sun-drying, the seed samples were ground into powder using a mixer grinder, and the particle size was prepared by using Indian Standard (IS) sieves less than 1 mm. The particle size of the sample plays a crucial role in the conversion process; it affects the impact of activation energy and heat transfer directly, i.e., smaller particle size required lower activation energy to start the conversion process and the higher the impact of heat transfer. The general overview of the representation of the characterization is outlined in Fig. 1.

Table 1 Taxonomy of the plant

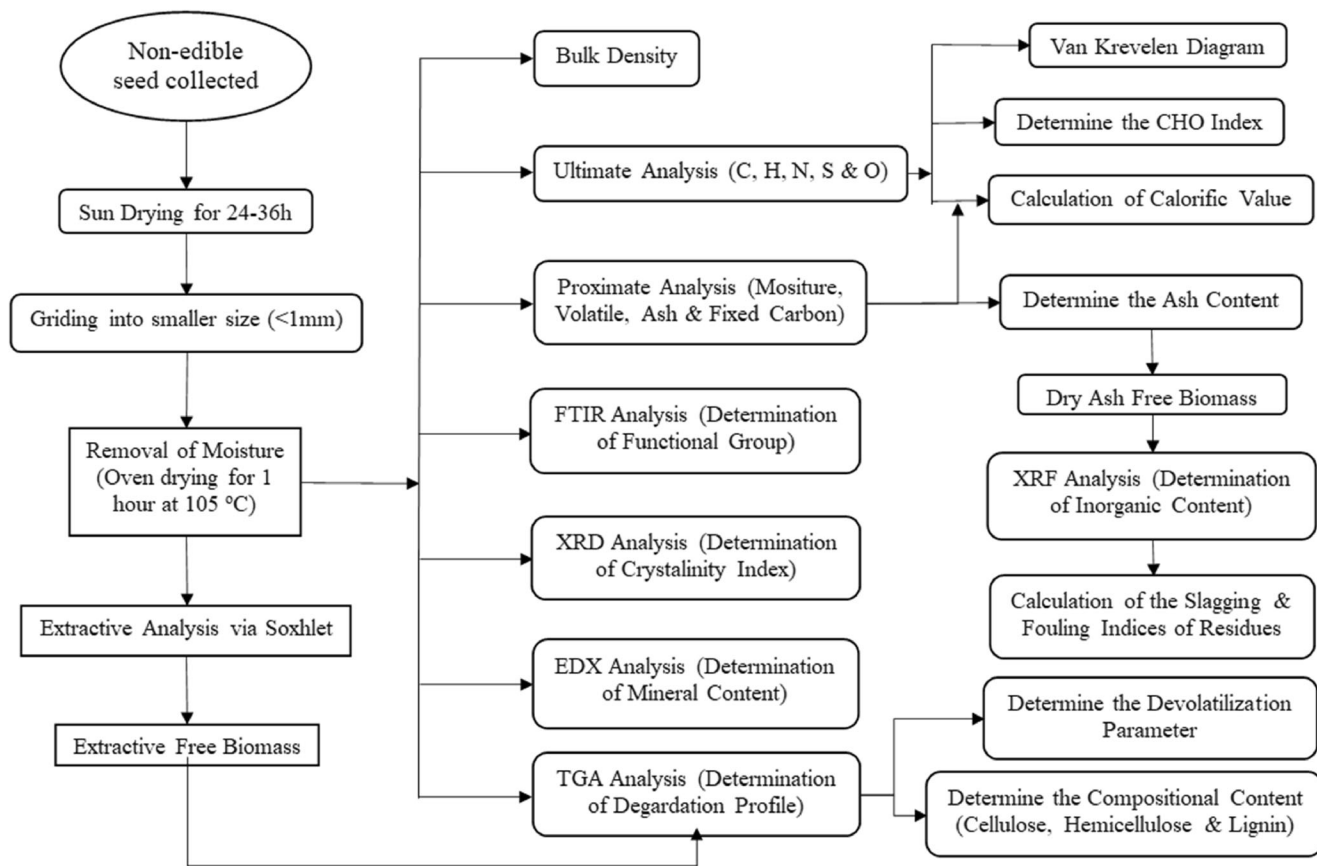| Plant name	Putranjiva	Amaltas	Siris
Kingdom	Plantae	Plantae	Plantae
Division	Tracheophyta	Mangoliophyta	Mangoliophyta
Class	Magnoliopsida	Magnoliopsida	Magnoliopsida
Order	Malpighiales	Fabales	Fabales
Family	Euphorbiaceae	Caesalpiniaceae	Mimosaceae
Genus	Putranjiva	Cassia	Albizia
Species	Roxburghii	Fistula	Lebbeck

Fig. 1 A detailed characterization scheme

2.2 Extractive and compositional analysis

For the analysis of extractives, the 3.0 g of moisture-free dried biomass samples were taken into a cellulose thimble (25 × 75 mm size) and placed into a Soxhlet apparatus for leaching process with 150 mL of each polar (ethanol) and non-polar (hexane) solvent. By using a heating mantle, the apparatus was heated at a moderate temperature (around 65 °C) for 5 h. After completion of hexane leaching process, the residual samples were dried at 70 °C for 3 h in a hot air oven to a constant weight. The dried samples were then cooled in a desiccator and measured. Additional hexane extractive-free dried biomass was transferred into the same apparatus and used a polar solvent to extract further. All soluble compounds such as terpenoids, non-polar lipid compounds, and hydrocarbons were extracted during the hexane leaching phase, while the residual chlorophylls, sterol, polar wax, and certain small compounds were extracted at the time of ethanol leaching process. Both of the solvents were recovered in a rota-evaporator by removing the extractives at around 60 °C under decreased pressure. Extractive-free samples were obtained from the cellulose thimble at the end of the extraction cycle and used to test composition such as hemicellulose, cellulose, and lignin based on their thermal degradation profile by TGA

study. Extractive content can be determined by using the given formula,

$$EC\ (\%) = \left[\frac{A}{B}\right] \times 100 \tag{1}$$

where A = weight of extractives, B = weight of oven-dried biomass, and EC = extractive content.

2.3 Proximate analysis

Proximate analysis is the early stage of the characterization process, which was done to determine the amount of moisture content (MC), ash content (AC), volatile matter (VM) content, fixed carbon (FC) content, and total solid (TS) content of biomass sample. The nature of the biomass materials is commonly hydrophilic. Hence, moisture removal of these materials becomes very necessary or else it will have a detrimental effect on the pyrolysis product yield. Five grams of sun-dried biomass samples were transferred into a glass petri dish and placed it into a hot air oven at 105 °C for 1 h. Moisture content is calculated by using the given formula,

$$MC\ (\%) = \left[\frac{A-B}{A}\right] \times 100 \tag{2}$$

where A = weight of a sample as received, B = weight oven-dried sample, and MC = moisture content.

Furthermore, 1.0 g of moisture-free biomass sample was taken in a crucible and placed into a muffle furnace at 570–580 °C for 4 h. Then the weight and the difference between the sample weight before and after (%w/w) give the ash content in percentage.

For the volatile matter estimating, 1.0 g of moisture-free biomass sample was taken in the same crucible with lid covered and placed it into a muffle furnace at 910–920 °C for 7 min. After that, the sample was cooled in a desiccator and weighed. The difference in weight loss gives the volatile matter content of the biomass. It can be determined by using the given formula,

$$\text{VM}(\%) = \left\{ \left[\frac{A-B}{A} \times 100\right] - \text{MC}(\%) \right\} \tag{3}$$

where A = weight of the sample before heating, B = weight of the sample after heating, MC = moisture content, and VM = volatile matter content.

Furthermore, the amount of fixed carbon content of the biomass sample was determined by the given below empirical equation,

$$\text{FC}(\%) = 100 - \text{MC}(\%) - \text{AC}(\%) - \text{VM}(\%) \tag{4}$$

where AC = ash content and FC = fixed carbon content.

The total solid content was estimated using the given formula,

$$\text{TS}(\%) = 100 - \text{MC}(\%) \tag{5}$$

where TS = total solid content and MC = moisture content.

2.4 Elemental analysis

Biomass material elemental processing was carried out on a dry basis (db) using CHNSO elemental analyser (Elementar, Vario EL III, Germany). It commonly reports the amount of carbon (C), hydrogen (H), nitrogen (N), sulphur (S), and oxygen (O) content of the samples. Five milligrams of accurately weighed samples were taken in a tin capsule and heated at a fixed temperature of 980 °C with a constant and continuous flow of helium-enriched oxygen gas. Further, given data were analyzed by using Callidus® software for the determination of the elemental composition of the given biomass sample.

2.5 Higher heating value (HHV)

Biomass heating value plays a crucial role in examining the potential of biomass to produce biofuel. With soil, minerals, and weather conditions, the heating value of the lignocellulosic biomass can differ considerably. The

HHV of biomass was determined according to the following empirical equation provided by the International Energy Agency (IEA) [12],

$$\begin{aligned}\text{HHV}\left(\frac{\text{MJ}}{\text{Kg}}\right) &= 0.3491 \times C(\%) + 1.1783 \times H(\%) \\ &\quad + 0.1005 \times S(\%) - 0.0151 \\ &\quad \times N(\%) - 0.1034 \times O(\%) - 0.0211 \\ &\quad \times \text{AC}(\%) \end{aligned} \tag{6}$$

where C, H, S, N, O, and AC are the amount of carbon, hydrogen, sulphur, nitrogen, oxygen, and ash, respectively.

2.6 Bulk density

Biomass bulk density is an important physical property in transport infrastructure and logistic network handling. It was defined as the proportion of the weight of the particles of biomass to the total volume of the particles of biomass, with the amount of pore space between and within the particles of biomass. It depends on the shape and size of the particles, moisture content, degree of fill tightness, and characteristics of the surface [13]. It has a direct relation with the storage and transportation cost. It has a direct impact on the size of the material, handling of material, the behaviour of the material during the conversion process, and storage requirements. It was evaluated and estimated using the method given by Obernberger and Thek [14]. In basic laboratory equilibrium, the volume and weight of the samples were determined. The volume of biomass was determined through the use of a graduated cylinder. For the reproducibility of the correct results, the experiment was replicated thrice, and mean results were recorded in this analysis.

2.7 Thermal conductivity

Biomass is a highly anisotropic material. In the thermochemical conversion processes, when biomass is heated, the particles of biomass are exposed to heat conduction along, and by their compositional structure, which in result affects their thermochemical conversion performance. The thermal characteristics of biomass significantly affect the process of conversion. It depends on moisture, density, temperature, heating direction, and porosity [15]. The given correlation equation can determine it,

$$K_{\text{eff}} = \{\text{sg}(0.2 + 0.0055 \times \text{MC}) + 0.0238\}, \text{MC} < 40\% \tag{7}$$

where K_{eff} = thermal conductivity of biomass, sg = specific gravity, and MC = moisture content.

2.8 CHO index

CHO index was defined as the oxidation state of organic carbon in organic resources. Benjamin F. Mann [16] proposed a given formula to determine the CHO index,

$$\text{CHO index} = \frac{2 \times [O] - [H]}{[C]} \tag{8}$$

where $[O]$, $[H]$, and $[C]$ are the mole fraction of oxygen, hydrogen, and carbon of the sample, respectively.

2.9 H/C_eff ratio

Biomass is hydrogen-deficient material. The intensive feature of biomass is essential for its conversion. The H/C_{eff} ratio has been determined to have a massive impact on the production of aromatics, olefins, and formation of coke during the catalytic cracking with zeolite [17]. This ratio also gives the idea of the rate of deactivation of the catalyst. The ratio can be estimated by the given formula,

$$H/C_{\text{eff}} = \frac{[H] - 2 \times [O] - 3 \times [N] - 2 \times [S]}{[C]} \tag{9}$$

where H, O, N, S, and C are the amounts of hydrogen, oxygen, nitrogen, sulphur, and carbon from the elemental analysis of biomass.

2.10 Van Krevelen plot

The Van Krevelen plot offers a method for visualization of the elemental variations in composition between the samples. The atomic proportion of hydrogen to carbon (H:C) and oxygen to carbon (O:C) was used for the visualization of the Van Krevelen diagram in this analysis. Hence, tracing the hydrocarbons becomes accessible in the biomass sample.

2.11 Biofuel reactivity

The reactivity of the biofuel was estimated from elemental and proximate analysis. It was obtained by dividing the volatile matter to fixed carbon content and the molar ratios of H/C and O/C in the samples.

2.12 XRD analysis

Using Rigaku TT Rax diffractometer along with 9 kW and 250 mA provided source of Cu-Kα radiation, the XRD pattern of the biomass samples was performed to identify crystallographic structure. The angle scanning speed (2θ) was taken at a pace of 1°/min from 5 to 50°. The provided equation defined the crystalline indices (CrI) of the biomass samples:

$$CrI\ (\%) = \left[\frac{I_{002} - I_{\text{amp}}}{I_{002}}\right] \times 100 \tag{10}$$

where I_{002} and I_{amp} are the intensity of crystallinity peak at $2\theta = 22.5$ (i.e., cellulose) and intensity of the amorphous peak at $2\theta = 16.5$ (i.e., cellulose, hemicellulose, and lignin) respectively. Broad peaks characterized the amorphous areas, while crystalline regions gave rise to narrower peaks.

2.12.1 FTIR analysis

Fourier transform infrared spectroscopy (Shimadzu Corpn., Japan, IR-Prestige 21) analysis was used to investigate the presence of various functional groups of the samples. A small amount of samples were mingled with dried KBr powder in a ratio of approximately 1:100 (%w/w) and loaded in the sample holder. The FTIR spectra were collected at 4 cm^{-1} resolution using an IR range of 400–4000 cm^{-1} and at a scanning pace of 15 scans/min in transmission mode.

2.12.2 EDX analysis

To examine the mineral contents of the raw seed samples, the Energy-dispersive Xray spectroscopy (EDX) was employed. FESEM/EDX (ZEISS, Sigma) was used for this study. A small amount of oven-dried samples were placed on a small piece of carbon tape for the analysis.

2.12.3 XRF analysis

To identify the inorganic elements (Fe_2O_3, CaO, MgO, K_2O, Na_2O, SiO_2, TiO_2, and Al_2O_3) of the residual biomass sample, the X-ray fluorescence spectrometer (Epsilon 1 PANalytical B.V.) was used in this study. Propensity to deposition of ash was represented by slagging and fouling indices, expressed as follows:

Base to acid ratio (B/A)

$$= \frac{\%[Fe_2O_3 + K_2O + Na_2O + MgO + CaO]}{\%[Al_2O_3 + SiO_2 + TiO_2]} \tag{11}$$

Sillica to alumina ratio (S/A) $= \dfrac{\%[SiO_2]}{\%[Al_2O_3]}$ (12)

Iron to calcium ratio (I/C) $= \dfrac{\%[Fe_2O_3]}{\%[CaO]}$ (13)

Total alkalis (TA) $= \%[Na_2O + K_2O]$ (14)

2.13 TGA analysis

To determine the thermal degradation and compositional content of dried seed materials and extractive-free dried seed

materials respectively were performed in simultaneous differential thermal analyzer (Model No. TG 209 F1 Libra; Make: M/s Netzsch, Germany), where simultaneous TG and DTG (derivative thermogravimetric) curves were obtained in the temperature range of 25 to 900 °C at a heating rate of 10 °C/min. In brief, 5–15 mg of biomass samples were taken into an alumina crucible and heated under nitrogen atmosphere, where rate of carrier gas flow (highly pure N_2) was set at 40 mL min^{-1} and 40 mL min^{-1}, respectively.

TG and DTG patterns were used to determine some vital parameters from the thermal performance of the biomass samples. To quantify the thermal performances of various biomasses, a comprehensive devolatilization index (D_i) has been defined by [18] as follows:

$$D_i = \frac{\left(\frac{dw}{dt}\right)_{max}\left(\frac{dw}{dt}\right)_{mean}}{T_{in}T_{mx}\Delta T_{0.5}} \tag{15}$$

where $(dw/dt)_{max}$ is the maximum mass loss rate according to DTG peak, $(dw/dt)_{mean}$ is the mean mass loss rate, T_{in} is the initial temperature, T_{mx} is the temperature of maximum degradation rate, and $\Delta T_{0.5}$ is the temperature range at when (dw/dt)/(dw/dt)$_{max}$ is equal to 0.5.

2.14 Kinetic analysis by single heating rate model

2.14.1 Broido (BR) method

Broido proposed an imprecise but direct mathematical model for determining the activation energy (E_a) at a single constant heating rate (β) of the pyrolysis process. In this method, the thermal degradation process is considered to be of first-order, and the calculations are done accordingly [19]. The following expression was used to compute the activation energy (E_a) concerning each stage of decomposition:

$$\ln\left[\ln\left(\frac{1}{Y}\right)\right] = -\frac{E_a}{RT} + \ln A \tag{16}$$

where,

$$Y = \frac{W_t - W_f}{W_i - W_f} \tag{17}$$

where, Y is the fraction of the number of initial molecules not yet decomposed; W_t is the weight at temperature t; W_f and W_i are denoted the final weight and initial weight of the sample, respectively. A plot between $\ln[\ln(1/Y)]$ vs. $1/T$ provides an excellent approximation to a straight line, and the slope $-E_a/R$ was used to evaluate the activation energy (E_a).

2.14.2 Horowitz-Metzger (HM) method

HM has demonstrated the method of calculation of activation energy (E_a) of biomass materials. In this case, the curve having the highest correlation coefficient values among the reaction of different orders is considered, but here, we are assuming only the first order of the reaction. The following expression proposed by the Horowitz and Metzger [20] was written:

$$\ln\left[\ln\left(\frac{1}{Y}\right)\right] = \frac{E_a\phi}{RT_{max}^2} \tag{18}$$

where, $\phi = T - T_{max}$, T is the temperature at particular weight loss, and T_{max} is the temperature at when the value of $1/Y$ is 2.718. The linear plot of $\ln[\ln(1/Y)]$ vs. ϕ gives an approximation to a straight line, and the energy of activation (E_a) was calculated from the slope of the straight path.

3 Results and discussion

### 3.1 Extractive and compositional content

The presence of the extractive was assessed using a polar and non-polar solvent by the soxhlet apparatus, and tabulated in (Table 2). From the results, it can be observed that PR seed bears more extractives or oils as compared to other reported seeds like Linseed [4], Sapodilla [5] and *Samanea saman* [21]. The AL (24.06%) and CF (18.83%) have less oil content than PR (50.55%). Hence, higher oil content in the seed sample produces more amount of liquid products during conversion or pyrolysis.

The thermal degradation behaviours of cellulose, hemicellulose, and lignin content in the extractive free seed samples were evaluated by thermogravimetric analysis which are shown in Fig. 2. Lignocellulosic composition influences the performance of the biomass pyrolysis. The temperature range of hemicellulose and cellulose degradation is 25–150 °C and 150–450 °C respectively, and temperature range for lignin degradation is 450–700 °C for all three extractive free seed samples. The higher amount of hemicellulose and cellulose with less lignin in the seed sample is good for rising the rate of thermal degradation during pyrolysis as hemicellulose and cellulose degrade at a lower temperature range, while lignin degrades at a higher temperature range [4]. It was observed that the lignin and hemicellulose contents of AL are closely similar to the CF, but the cellulose content is different. CF has less cellulosic material of 56.67% than PR (60.82%) and AL (60.6%). The amount of total chemical content varied from 70 to 75% (Table 2) and decreased in the order of PR (74.54%) > AL (73.78%) > CF (70.01%).

Table 2 Details characterization of PR, CF, and AL with other reported biomass

Biomass	PR	CF	AL	Linseed [4]	*Samanea saman* [20]	Sapodilla [5]
			Proximate analysis			
MC(%)	3.81	6.26	6.55	6.53	6.19	8.07
AC(%)	5.68	6.03	4.63	10.5	3.06	1.19
VM(%)	86.25	79.65	83.69	76.95	76	77.02
FC(%)	4.26	8.06	5.12	6.02	14.74	13.73
TS(%)	96.19	93.74	93.44	93.47	93.81	91.93
VM/FC(%)	20.25	9.88	16.34	12.78	5.156	5.61
Ultimate analysis						
C(%)	51.96	42.37	42.97	61	48.46	52.67
H(%)	9.24	7.51	7.79	8.5	6.75	6.74
N(%)	0.74	2.98	6.09	3	7.3	1.46
S(%)	0.86	0.39	0.71	0.3	–	0.34
O(%)	37.19	46.74	42.44	27.2	37.47	38.78
O/C molar ratio	0.53	0.83	0.74	0.004	0.58	0.55
H/C molar ratio	2.12	2.11	2.16	1.66	1.67	1.54
C/N molar ratio	81	16.56	8.23	–	–	–
HHV (MJ/Kg)	25.14	18.68	19.67	27.9	17.68	20.05
Bulk density (kg/cm^3)	411.4	585.2	549.5	–	657.41	454.3
Chemical analysis (%)	74.54	70.01	73.78	81.6	67.95	68.19
Hemicellulose (%)	6.09	7.12	7.05	11.9	26.55	26.55
Cellulose (%)	60.82	56.67	60.6	49.4	30.81	34.03
Lignin (%)	7.63	6.22	6.13	20.3	10.59	7.61
Total extractive (%)	50.55	18.83	24.06	33.55	30.66	29.84
Hexane (%)	34.21	12.69	10.19	32.62	9.86	25.44
Ethanol (%)	16.34	6.136	13.87	0.93	20.8	4.4
H/Ceff	0.99	0.27	0.3	–	0.11	0.34
CHO index	1.07	1.85	1.61	–	1.26	1.21
K_{eff} (w/mK)	0.11	0.16	0.15	–	–	–
Empirical formula	$C_{86.4}H_{183.2}O_{46.4}NS_{0.4}$	$C_{16.76}H_{35.47}O_{13.9}NS_{0.04}$	$C_{8.3}H_{17.97}O_{6.16}NS_{0.04}$	–	–	–

Fig. 2 TG-DTG curves of extractive-free seed materials
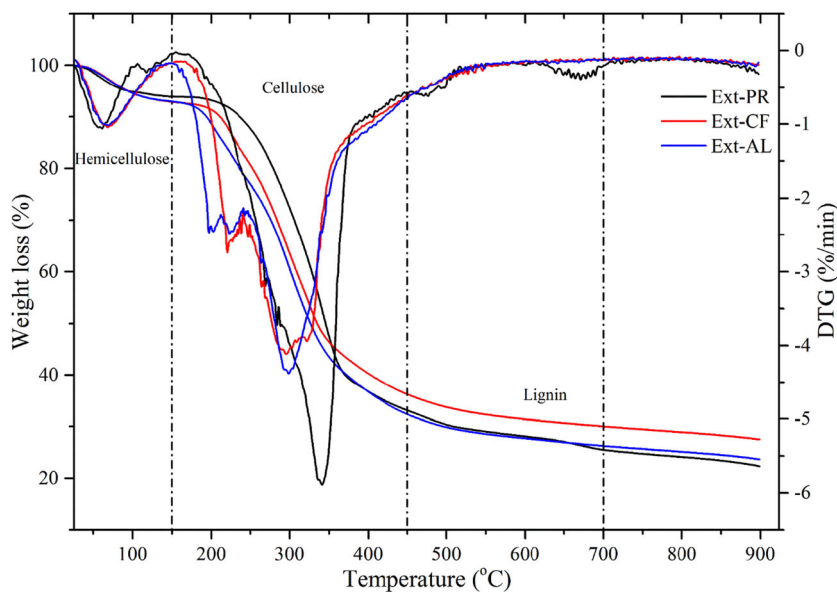
3.2 Proximate analysis

The proximate analysis gives an understanding of the excellent heating and burning properties of seed samples. The results of this study and other non-edible oilseeds are tabulated in (Table 2). The existence of higher moisture content in the biomass sample usually reduces the heating value of the feedstock and adversely affects the quality of the pyrolysis products, mainly bio-oil [22]. Nearly all raw seed samples contain a lesser amount of moisture (3.0–7.0%). CF and AL contain 6.26% and 6.55% of moisture, respectively, which was higher than PR (3.81%). Hence, PR has the highest heating value as compared to CF and AL. It was observed that the ash content present in AL (4.63%) was lower than PR (5.67%) and CF (6.03%) biomass. The ash content of the sample relies upon the soil, climate, and geometry (places) where the plant grows up. Due to the presence of soluble ionic compounds and organic materials in the ash of biomass, it acts as a catalyst during gasification and pyrolysis [23]. In the present study, ash content of CF seed was found to be higher, resulting in a lower heating value compared to AL as lowering the ash content means higher the heating value [24]. But among all three seed samples, the highest heating value was observed in PR due to its very less moisture content. The result of proximate analysis also shows that the volatile matter content in the three biomasses analyzed varied from 79.50 to 86.50% (Table 2) and improved by CF (79.65%) < AL (83.69%) < PR (86.25%). The volatile matter content present in biomass affects the reactivity of the fuel. Higher volatile matter content suggests fast fuel ignition. The amount of fixed carbon was much higher in CF (8.06%), corresponding to the lowest volatile matter content, 79.65%, which might be due to the presence of high amount of silica which confirms from the EDX result in section 3.9 of this paper. Fixed carbon of the seed sample often contributes to the heating value of any fuel, and it serves as the primary heat producer during burning. Fixed carbon was lowest for PR (4.26%) with the highest amount of total solid content, 96.19%. Results from proximate analysis of the present sample suggested that these biomasses can be ignited even at low temperatures with a higher heat transfer rate [25].

3.3 Elemental analysis

Summarized data of elemental analysis of the present study, along with other seed samples are tabulated in Table 2. It is beneficial in assessing the amount of air needed for combustion. The carbon content in biomass is directly related to the heating value, and the oxygen content has an inverse relation to the heating value which implies a higher carbon content, and a lower oxygen must lead to a higher heating value [5]. The carbon content was much higher in PR (51.96%), corresponding to lower oxygen content, 37.19%, which resulted in

higher heating value (Table 2). Hydrogen was found in the range of (7.5–7.8%) except PR (9.24%). The nitrogen and sulfur content of all the seed samples analyzed was in the range (0.7–6.1%) and (0.39–0.86%), respectively, which indicated minimum NO_x and SO_x emissions during pyrolysis and reduced corrosion problems in boiler and pipelines also. The oxygen content varied from 37.20–46.75% (Table 2) and decreased in the order of CF (46.74%) > AL (42.44%) > PR (37.19%). Thus, these findings can help in screening favorable catalysts for removing oxygen and heteroatom from bio-oil derived from these non-edible seeds during pyrolysis. The C/N ratio influence the rate of decomposition rate which means higher C/N ratio leads to a decreased decomposition rate [26]. In present study, it was noticed that AL seeds have lower C/N ratio (8.23%) which may favor faster decomposition by microorganisms [27].

3.4 Higher heating value and bulk density

The higher heating value depends upon both proximate and elemental analysis of the biomass materials. The HHV deals with conditions where water is condensed out of the combustion products. From Table 2, it was found that higher heating values varied from 18.68 to 25.14 MJ/Kg, which was calculated by using Eq. (6). The minimum heating value was recorded in CF (18.68 MJ/Kg) which was attributed to the existence of minimum amount of carbon (42.37%) and hydrogen (7.51%) and also maximum oxygen (46.74%) and ash (6.03%) content. The maximum heating value was found in PR (25.14 MJ/Kg) due to the lowest % of oxygen (37.19%) and maximum carbon (51.96%) content. Similarly, heating value of 27.9 MJ/Kg was obtained with carbon 61% and oxygen 27.2% from the ultimate analysis of linseed [4].

Bulk density of different seed samples showed less variation; the minimum was found in PR (411.36 Kg/m^3), and the maximum was recorded in CF (585.17 Kg/m^3) from Table 2. Higher the bulk density of biomass would be less challenging for storage, handling, and transportation. Results revealed that the bulk density of all the seed materials was in the same range as that of reported biomass such as Sapodilla (454.26%) [5] and *Samanea saman* (657.41%) [21].

3.5 Thermal conductivity, CHO index, and H/C_{eff} ratio

The thermal conductivity of biomass is a fundamental parameter for distinguishing the capability of heat transfer. From Table 2, it was found that, the thermal conductivity was varied from 0.11 to 0.16 w/mK and increased in order of PR (0.11 w/mK) < AL (0.15 w/mK) < CF (0.16 w/mK). Moisture content has a direct association with the thermal conductivity of the biomass materials, which means higher the moisture content, higher the thermal conductivity of the materials.

The CHO index can vary from -4.0 to $+4.0$. From Table 2, CF showed the highest CHO index (1.85), which credits to increasingly oxidized compounds, while PR showed the lowest CHO index (1.07), which indicates reduced molecules of oxidized compounds. A $+ve$ sign value in the CHO index demonstrates that the oxygen content of the sample is generally high, while hydrogen content is moderately low, which directly affects the heating value of that sample. Higher the CHO index signifies lower the heating value. Also, it was confirmed that CF has a lower heating value (18.68 MJ/Kg) as compared to PR (25.14 MJ/Kg).

H/C_{eff} ratio was calculated by using Eq. (9) and presented in Table 2. It was varied from 0.27 to 0.99 and increased in the order of CF (0.27) < AL (0.30) < PR (0.99). It has a direct association with CHO index and heating value likewise, which means higher the H/C_{eff} proportion, higher the heating value, and lower the CHO index. The H/C_{eff} ratio has a direct impact on the stability of the catalyst due to low coke accumulation during the catalytic pyrolysis of biomass. It is feasible to use feedstock with a high H/C_{eff} ratio (≥ 1.0) to provide hydrogen to the hydrocarbon pool for feedstock conversion [28]. It was observed that PR has a good H/C_{eff} ratio (~ 1.0) value, which means it may perform better during catalytic pyrolysis, followed by CF and AL.

3.6 Van Krevelen diagram and biofuel reactivity

The Van Krevelen diagram demonstrates the degree of carbonation and aromaticity in the biomass and heating value of feeds also [4], which is represented in Fig. 3a. It was affirmed that the H/C proportion was in the scope of 2.11–2.16 with O/C proportion going from ~ 0.5–0.8, which has been discovered to be as solid as other disclosed biomass in Table 2. Higher H/C proportion of seed sample indicated as fast ignited fuel. From the data in Table 2, among all seed samples, AL has easy burning efficiency due to higher H/C proportion (2.16). The H/C and O/C proportions in PR were lower than AL, which was due to dehydration and decarboxylation. The literature revealed that with high H/C and low O/C proportions showing a higher quality liquid product during pyrolysis [29].

Biofuel reactivity concerns the estimation of the molar ratios of VM/FC, H/C, and O/C for all seed samples and shown in Fig. 3b. The ratio of VM/FC was much higher in PR (20.25), corresponding to the lowest H/C and O/C ratios, 2.12 and 0.53. The ratio of VM/FC varied from ~ 9–20 (Table 2) and increased in the order of CF (9.88) < AL (16.34) < PR (20.25). Interestingly, VM/FC ratios of all the seed samples were found to be higher and reactive than other reported biomass viz. *Samanea saman* [21], *Jatropha curcas* [7]. Thus, these seed samples signified a better advantage for their utilization as solid fuel and liquid fuels.

3.7 XRD analysis

The XRD pattern of all the seed samples, as appeared in Fig. 4a shows the presence of crystalline peaks and amorphous peaks. The cellulose crystallinity has a significant impact on the thermal degradation profile. The thermal degradation temperature was reduced due to lower crystallinity [5]. In some literature, it was postulated that biomass crystallinity relies upon wax substances. It has likewise been accounted for that crystalline cellulose produces less gas and char when contrasted with amorphous cellulose, which contributes less to the levoglucosan during pyrolysis [30]. Using the diffractometers pattern, the CrI values were calculated by using Eq. 10. In Fig. 4a, it was observed that there is no sharp peak for CF and PR; therefore, amorphous phase is present. The CrI values were found in the case of AL (43.92%). The obtained CrI values of AL biomass were differed fundamentally with other revealed biomass, like, Mahua and Sapodilla [4, 5].

3.8 FTIR analysis

The FTIR analysis shows the auxiliary characterization of seeds. The transmittance spectra vs. wavenumber have appeared in Fig. 4b indicates the existence of alkane, alkene, carbonyl functional groups, and aromatic rings. The peak 3300–3310 cm^{-1} demonstrated the presence of aromatics, protein, phenols, alcohols, fiber, and water and is attributed to the stretching of abundant hydroxyl groups [5]. The peak of 2920–2930 cm^{-1} attributed to aliphatic C–H stretching indicated the presence of hemicellulose, cellulose, and lignin [6]. Peak 2855 cm^{-1} was due to the vibration of O–CH$_3$, which is usually present in lignin as can be found in the FTIR range of PR because of its high lignin content among all seed materials. The presence of carbonyl groups like ketones, carboxylic acid, and the ester (C=O) is seen at 1740 cm^{-1} due to p-coumaric acids of lignin and acetyl group of hemicellulose. The peak of 1650–1540 cm^{-1} ascribed to the presence of C=C aromatic ring stretching and the N–H amines groups. The aromatic methyl group vibration was observed in the peak allotted at 1462–1458 cm^{-1} because of the presence of cellulose and hemicellulose. The peaks found at 1235 cm^{-1} have signified the presence of the aryl group in lignin. The peaks at $\sim$ 1165 cm^{-1} and $\sim$ 1320 cm^{-1} were related to C–O–C stretching and –CH$_2$ wagging, respectively, present in cellulose and hemicellulose network. The peaks detected at 1050–1060 cm^{-1} alludes to the stretching of C–O due to the presence of polysaccharides and lignin. The heights of 870 cm^{-1} implied the presence of β-glycoside linkage, which is symmetric in polysaccharides and to the amorphous cellulose. At the lower peak region $\sim$ 790–490 cm^{-1} associated with the C–H out of plane twisting due to the presence of sugars like galactan, B-D fructose, and arabinan [6].
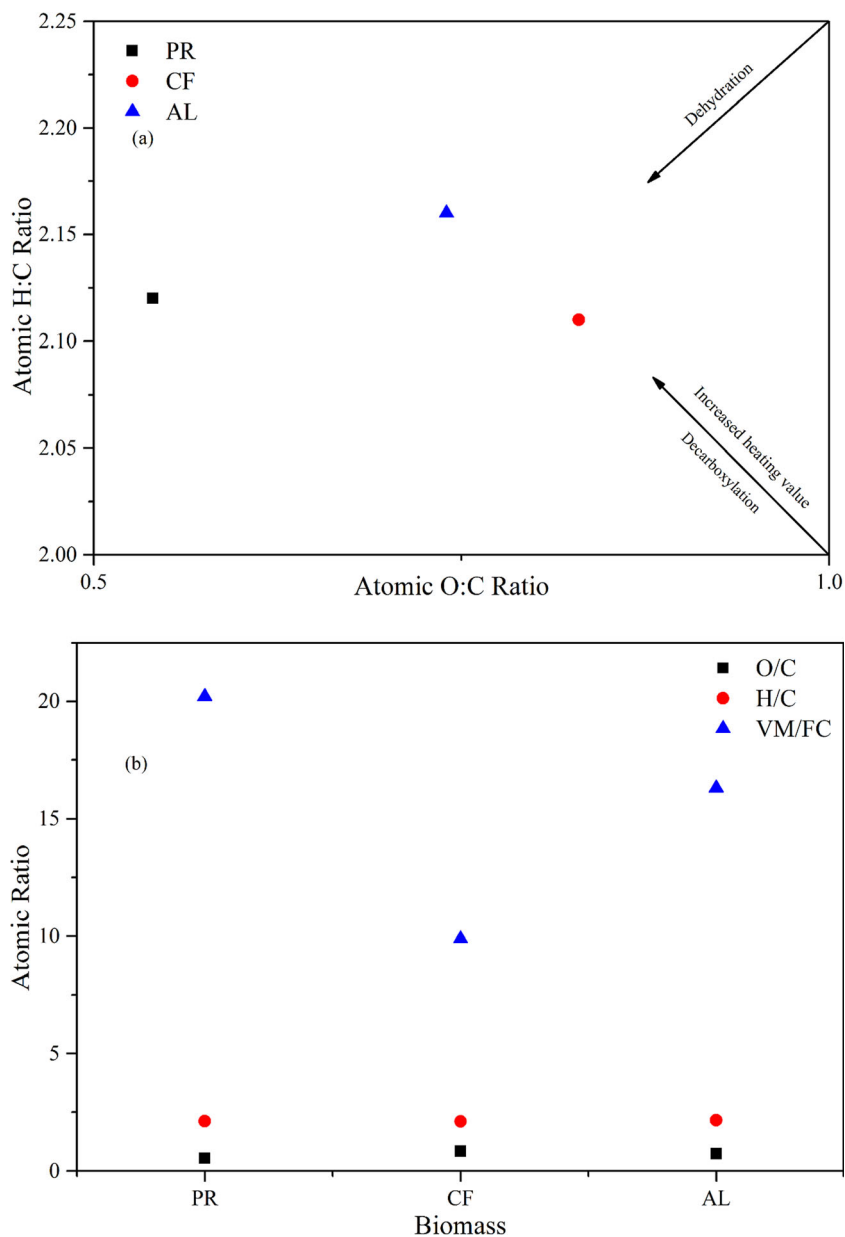
3.9 EDX analysis

The presence of mineral matter in the seed materials has played a vital role and provided positive effects on the pyrolysis and combustion process. Due to the presence of these minerals, they ascribed to upgrade the catalytic effect, which additionally increases the rate of conversion during pyrolysis. From Table 3, it was observed that PR (12.1%) has a maximum amount of Ca content than CF (6.4%) and AL (1.9%) which acts as a catalyst during pyrolysis. The presence of potassium (K) signified the frothing impacts during pyrolysis and increased the conversion rate; it was seen that the CF (32.6%) has the highest potassium (K) content as compared to others. It was likewise postulated that potassium (K)

catalysts upgrade the reaction rate because of their movement to active sites of free carbon [31]. Due to the presence of the maximum amount of silica (Si) in CF (19.1%), the fixed carbon content of CF was much higher among all the seed materials. From the results, it was observed that a small amount of lead (Pb) was found in all seed materials. Presence of lead (Pb) in the biomass sample was eliminated to the environment during pyrolysis process [32]. Presence of Cu and Pb in biomass support in decreasing the activation energy to promote the pyrolysis process by producing more volatiles in both, gas and liquid phase [33]. It was revealed that the presence of copper (Cu) in the biomass promotes the production of aromatics to enhance the bio-oil yield than the gas yield and decrease the oxygen content in the bio-oil [34]. In the present

Fig. 4 **a** XRD pattern of raw seed materials. **b** FTIR spectra of raw seed materials
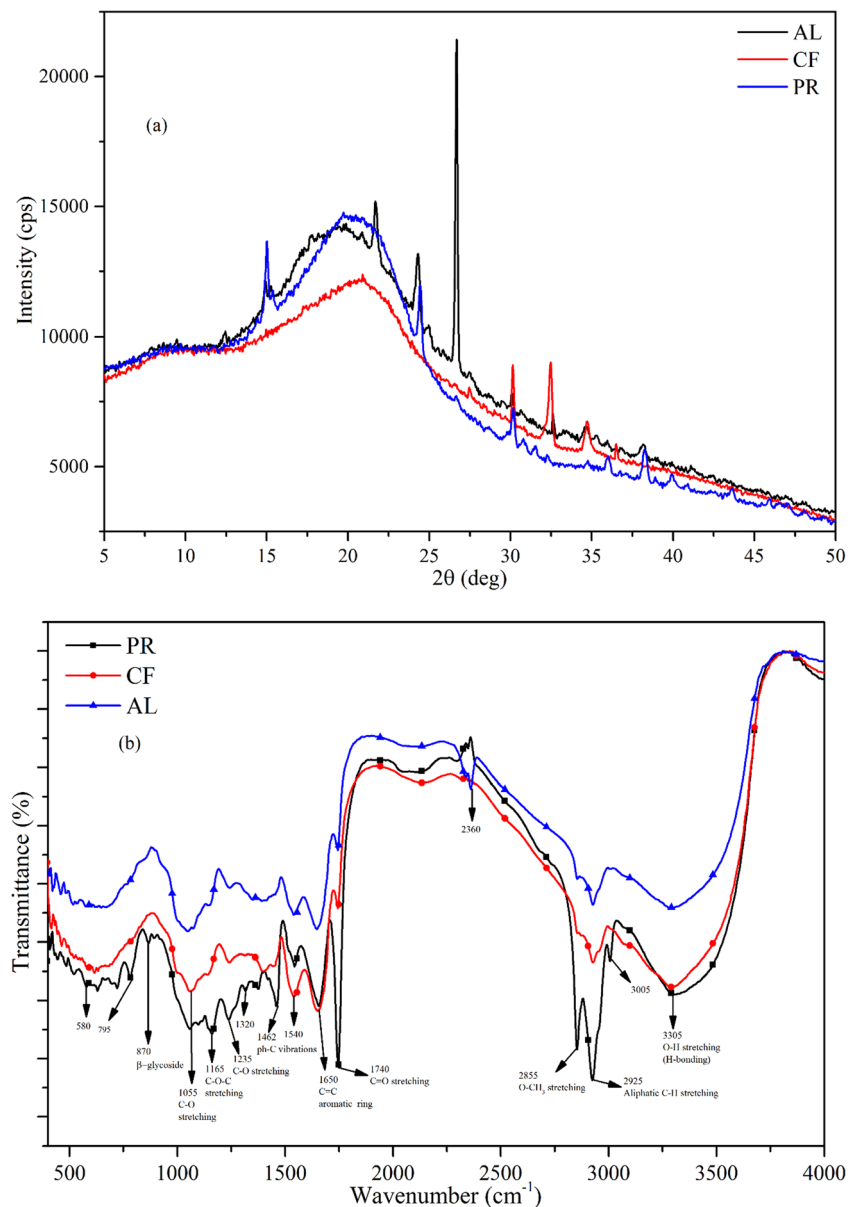
study, only Cu was found in AL (3.9%). For the most part, solid biomass feedstocks implied maximum percentage of Al, K, P, Ca, Mg, and Si alongside the little measure of different minerals, for example, Co, Ti, Mn, Cl, Na, Ni, and Fe. The mineral contents of the biomass varied little much, and different minerals are found due to the weather and soil conditions where the plant has grown.

3.10 XRF analysis

The XRF analysis of the residual seed materials is tabulated in Table 4, which were fundamentally same as other biomass. The slagging and fouling indices predictions were dependent on the inorganic composition of residual biomasses, which is represented in Table 5. Deposition propensities were determined by utilizing the Eqs. 11–14, which was given by A.M. Carpenter [35]. Few criteria can define the deposition propensity; for instance, when the values of B/A are > 1, in between 0.5 and 1.0, and < 1 indicates the deposition propensity is high, medium, and low, respectively. Moreover, when the values < 0.31 or > 3 of S/A and I/C proportion deposition propensity is generally low, while for values 0.3 < S/A or I/C < 3 deposition propensity is high. At the point when the values of S are < 0.6, in between 0.6 and 2, and > 2 signifies that the deposition propensity is relatively low, medium, and high, respectively. Similarly, when the values of TA are > 0.4, in between 0.3 and 0.4, and < 0.3 suggests that the fouling propensity is high, medium, and low, respectively. From the results, it was observed that due to the presence of high silica in AL residues, the deposition propensity was also high, and in

Table 3 EDX analysis of raw seed materials

Elements	PR	CF	AL
Al	53	7.6	40
F	–	–	21.9
K	11.4	32.6	11.4
Pb	7.6	3.5	5.8
Cu	–	–	3.9
Fe	3.5	0.5	3.9
Mg	1.1	6.3	3
P	–	18.1	2.7
Ca	12.1	6.4	1.9
Co	3	0.3	1.3
Na	0.9	0.8	1.1
Cl	0.8	1.4	1
Si	0.4	19.1	0.9
Ni	–	–	0.9
Cr	–	–	0.2
Mn	4.8	3.3	0.1
Ti	1.5	0.3	–

the case of PR and CF, the deposition propensity was medium and low, respectively. It was shown that ash-related issues ought to be relied upon in boilers because of high amounts of alkali in the present seed material residues, which generates

Table 4 XRF analysis of residual seed materials

Major elements	PR	CF	AL
SiO_2	0.717	0.106	2.953
Al_2O_3	0.0048	0.0035	0.002
CaO	34.994	34.357	28.999
TiO_2	0.066	0.045	0.15
P_2O_5	9.965	14.676	20.064
Na_2O	0.045	0.04	0.055
MnO	0.087	0.403	0.169
MgO	23.43	5.325	4.706
Fe_2O_3	0.535	0.508	1.587
Cl	0.186	0.196	0.685
K_2O	28.583	43.022	39.577
SO_3	0.77	0.57	0.076
Minor elements			
CuO	0.373	0.195	0.611
ZnO	0.086	0.189	0.164
Rb_2O	0.038	0.18	0.038
SrO	0.062	0.138	0.022
PbO	0.068	0.047	0.144

Table 5 Slagging and fouling indices

| Biomass	B/A	S/A	I/C	TA
PR	111.18	149.38	0.015	28.63
CF	538.85	30.286	0.015	43.06
AL	24.13	1477	0.055	39.63

molten salts via condensation, vaporization, and also high acid-to-base ratio [36]. However, these high fouling and corrosion issues can be settled in appropriate checking and control of the blowing system, which is financially accessible and can significantly assist with streamlining of the blower activities and the control of slag depositions.

Additionally, due to the presence of lower pyrite and quartz levels, these biomasses and their deposits are less corrosive and destructive relative to conventional fuels. Co-burning these biomasses with petroleum products is the most effective option for addressing these obstacles and improving industrial growth and a prominent way of utilizing biomass. It was noteworthy to notice that the TA of CF has relatively maximum among all biomass. The reaction in between alkali metal and silica present in deposits enables the generation of clingy fluid, which further prompts blockage of the air route of boiler and furnaces [37]. Finally, the present study has shown good agreement, alongside other revealed biomass [5, 7].

3.11 TG-DTG analysis

Pyrolysis process can convert lignocellulosic biomass efficiently into a variety of eco-friendly and value-added products, but the prediction of the product quality usually depends on the thermal degradation behaviour of the feed materials. Further, the pyrolysis characteristics of the seed samples were investigated by TG analysis. The detailed thermogravimetric analysis (TG) and the corresponding differential analysis of TG (DTG) of all seed materials are presented in Fig. 5a, b respectively. It was observed from the thermographs of seed materials that the thermal degradations were stepwise mechanisms and mainly occurred in three stages (dehydration zone, devolatilization zone, and char formation zone) that can be explained from their chemical composition. The first weight-loss stage, i.e., dehydration zone (< 200 °C) was due to the evaporation of moisture and loss of light volatile compounds. The second weight-loss stage, i.e., devolatilization zone (within 150 to 500 °C), was the one in which significant weight-loss was noticed mostly related to the pyrolysis of hemicellulose and cellulose in seed materials. This stage was also called the active pyrolytic region due to the maximum volatilization of biomass. In this stage, the aliphatic chains were broken, and

Fig. 5 Thermographs of raw seed materials. **a** TG curves. **b** DTG curves
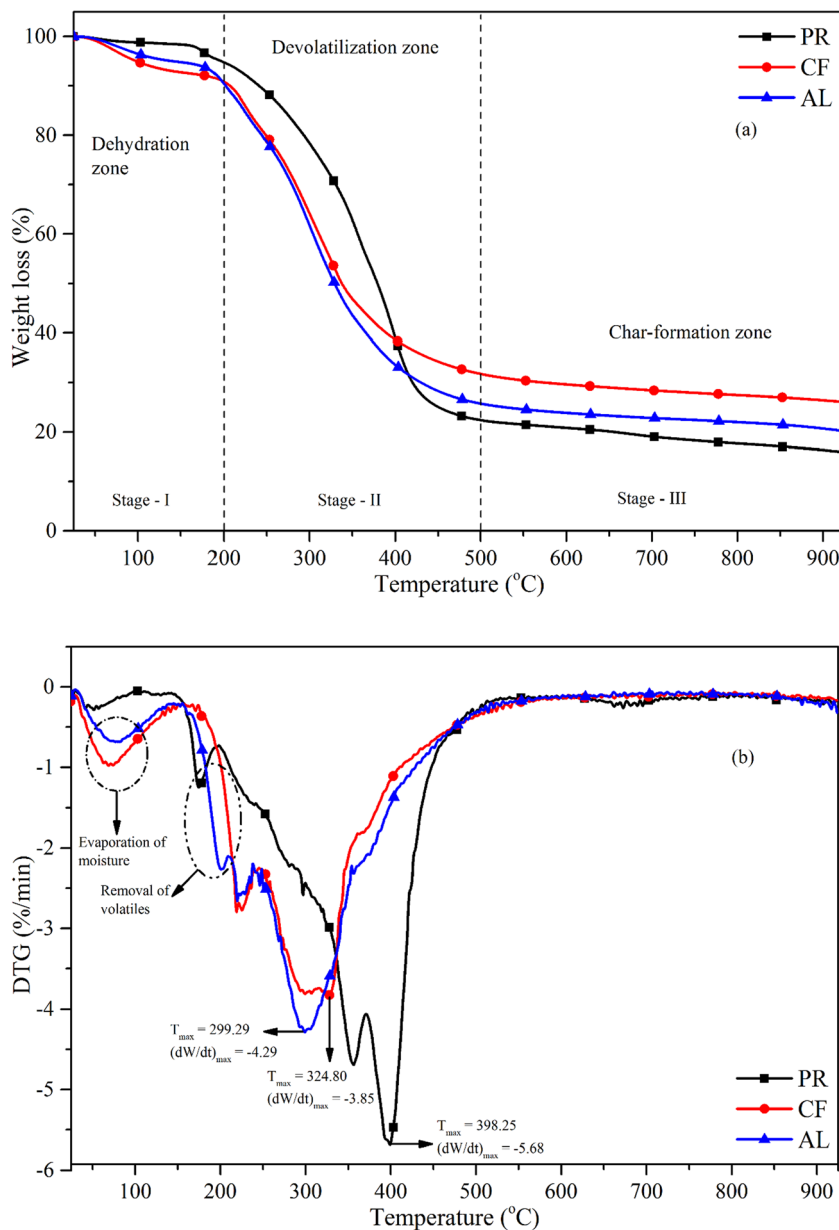
small gaseous molecules are formed. Finally, the third weight-loss stage, i.e., the char-formation zone (> 500 °C), occurred mainly due to the thermal degradation of lignin and hydroxyl phenolic groups. Among the three main components of biomass, lignin is the toughest one to be pyrolyzed, while hemicellulose is the easiest one followed by cellulose [38].

Table 6 Pyrolysis characterization from thermographs of raw seed materials

Biomass	T_{in} (°C)	T_{fi} (°C)	T_{mx} (°C)	$\Delta T_{0.5}$ (°C)	$(dw/dt)_{max}$ (%/min)	$(dw/dt)_{mean}$ (%/min)	W_t (%)	D_i
PR	229.58	412.49	398.25	76.50	− 5.68	− 0.93	84.07	7.55
CF	155.34	384.01	324.80	113.11	− 3.85	− 0.82	73.92	5.53
AL	192.06	384.74	299.29	86.17	− 4.29	− 0.88	79.79	7.62

With regard to the differential TG (DTG) curves (Fig. 5a, b), it was noticed that the rapid degradation of all seed materials occurred when the temperature was higher than 200 °C. The first degradation peak of DTG was obtained due to the evaporation of moisture and some extractives at the temperature up to 150 °C. Some extractives such as sugars, fats, pigments, and starches are thermally unstable, and they always lead a peak at low temperatures (< 150 °C) in DTG curves [39]. After that, a small peak showed up because of the expulsion of lighter volatile mixes and some non-polar lipid compounds at the temperature range of 150–200 °C. The degradation between 200 and 250 °C was mostly caused by the presence of hemicellulose and other minor compounds. The hemicellulose has a short molecular chain with many branches, and it quickly decomposed during the pyrolysis process. The most extreme degradation peak has happened in the temperature range of 250–500 °C because of the presence of cellulose and the evolution of major volatile components from the pyrolysis of these seed materials. Due to the linear and unbranched structure of cellulose, this contributes to better thermal stability. Furthermore, the lignin degrades gradually after 500 °C; it is tough to decompose during the pyrolysis process due to the presence of cross-linked aromatic rings.

The detailed pyrolysis characteristic parameters from the thermal degradation curves are presented in Table 6. It was signified that the initial temperature (T_{in}) is the prime indicator of the thermal stability of biomass, which means the higher T_{in}, the better the thermal stability. Hence, the thermal stability of PR (229.58 °C) was better than that of AL (192.06 °C) and CF (155.34 °C). Lower thermal stability means more ease in the pyrolysis process, which in turn suggested that the pyrolysis of CF occurred with relatively more ease followed by AL and PR. Moreover, the total weight loss (M_t) varied from ~73–84% (Table 6) and increased in the order of CF (73.92%) < AL (79.79%) < PR (84.07%). It was indicated that the residual char yield of PR was less followed by AL and CF. Furthermore, the volatile release characteristic index (D_i) indicated that the higher the D_i value means easier releasing of volatiles during the pyrolysis. The D_i value was much higher in AL (7.62 × 10^{-7}% min^{-1} °C^{-3}) corresponding to the lower T_{mx} value, 299.29 °C. The peak temperature range varied from ~300 to 400 °C (Table 6) and decreased in the order of PR (398.25 °C) > CF (324.80 °C) > AL (299.29 °C).

3.12 Kinetic analysis

Kinetic investigation of these seed samples was carried out by using the Broido and Horowitz-Metzger methods

Table 7 Kinetic study of PR, CF, and AL

Biomass	E_a (kJ/mol) by BR method	E_a (kJ/mol) by HM method
PR	34.46	56.26
CF	25.72	38.73
AL	30.14	42.95

and presented in Table 7. The activation energy (E_a) observed was in the order of PR > AL > CF by both the methods (Table 7). Results indicated that the maximum activation energy was found in PR (34.46 KJ/mol by BR method and 56.26 KJ/mol by HM method), followed by AL and CF. Product formation is considered to be a single-step reaction; thus, the method is assumed to be imprecise and straightforward representation to the actual kinetics of the system. The activation energy assessed via Broido's plot reiterates the fact that the pyrolysis reaction of these seed samples is complex, and there is need for several mathematical models to determine the system's kinetic parameters [40]. From Fig. 6a, b, it was observed that the correlation coefficient (R^2) values were good in Broido's plot as compared to Horowitz-Metzger's plot. The results obtained by the two methods are comparable except in a few cases, as none of these methods are perfect ones concerning assumptions as well as mathematical approaches. It was noticed that the initial temperature which was obtained from the thermographs of these seed materials has a direct relationship with the activation energy, which signified that the lower the activation energy, faster was the decomposition. Here, the activation energy (E_a) values were much lower in CF (25.72 KJ/mol by BR method and 38.73 KJ/mol by HW method) corresponding to the lowest T_{in}, 155.34 °C as followed by AL and PR. Lastly, these results align well with other studies which reported in the literature [5, 40].

4 Conclusion

The present work reports the comprehensive characterization of three different non-edible lignocellulosic biomass to elucidate their biofuel production potential for the pyrolysis process. It was found that all these seed materials contained a lower % of moisture (3.81–6.55%), which indicates a less negative impact on the bio-oil quality as well as heating value. PR may perform better in zeolite cracking as compared to CF and AL due to the high amount of H/C_{eff} ratio. Results reported herein clearly signified that due to the high amount of extractive

Fig. 6 Kinetic study plots (**a**) Broido method (**b**) Horowitz-Metzger method
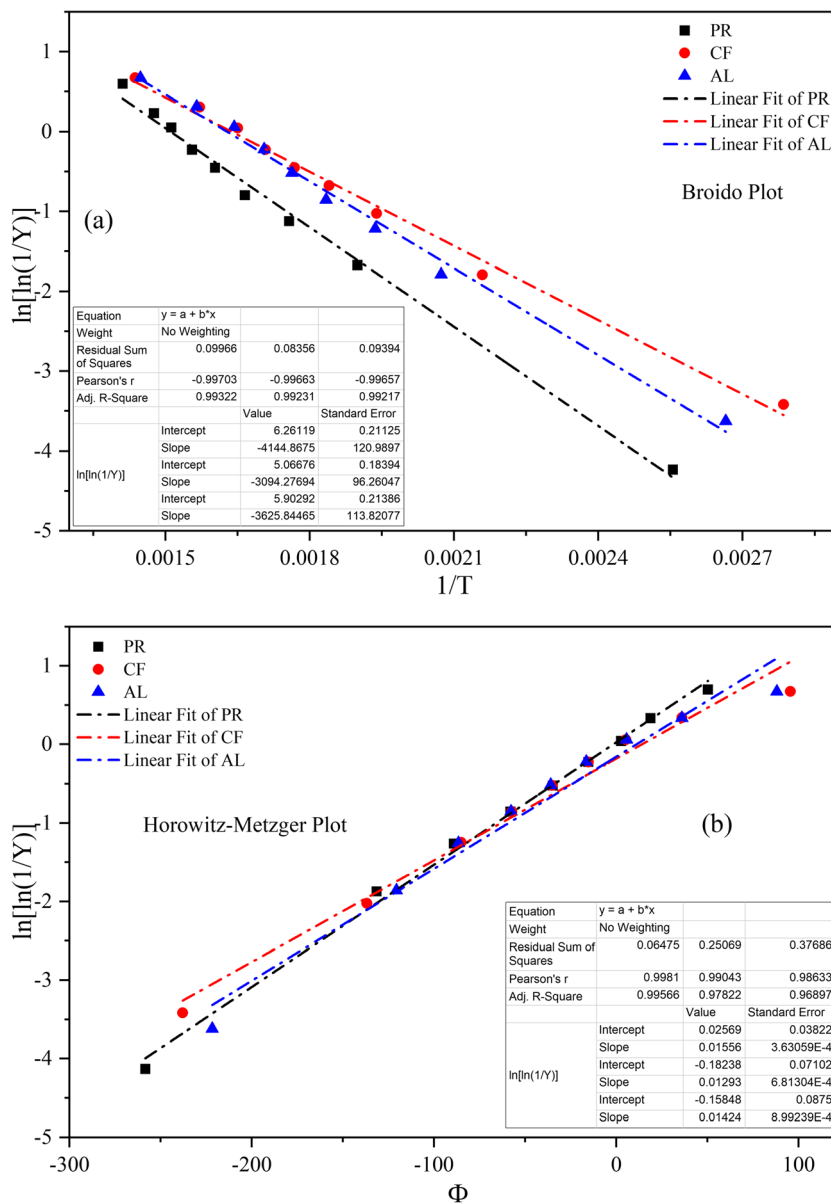
contents in these seed materials along with the lower amount of lignin content, these are suitable feedstocks for biofuel production with less char formation during pyrolysis. The activation energy (E_a) indicated that the CF decomposed faster than AL and PR. From the present study, it suggests that all these seed materials have an exceptional ability for the production of biofuels and some value-added chemicals via the pyrolysis process.

Nomenclature GHG, Greenhouse gas; PR, Putrunjiva roxburghii; CF, Cassia fistula; AL, Albizia lebbeck; TGA, Thermogravimetric analyser; DTG, Derivative of thermogravimetric analysis; FTIR, Fourier transform infrared spectroscopy; XRD, X-ray diffractometer; EDX, Energy-dispersive X-ray spectroscopy; XRF, X-ray fluorescence; EC, Extractive content; MC, Moisture content; AC, Ash content; VM, Volatile matter; FC, Fixed carbon; TS, Total solid; HHV, Higher heating value; K_{eff}, Thermal

conductivity; CrI, Crystalline indices; T_{in}, Initial temperature; T_{fi}, Final temperature; T_{mx}, Peak temperature; D_i, Devolatilization index; W_t, Total weight-loss; E_a, Activation energy; R, Ideal gas constant; T, Temperature; $(dw/dt)_{max}$, Maximum mass loss rate; $(dw/dt)_{mean}$, Mean mass loss rate; BR, Broido; HW, Horowitz-Metzger

References

1. OECD (2018) World Energy Outlook 2018. https://www.oecd-ilibrary.org/energy/world-energy-outlook-2018_weo-2018-en. Accessed 06 Sept 2019
2. BP Statistical Review of World Energy (2018) https://www.bp.com/content/dam/bp/business-sites/en/global/corporate/pdfs/energy-economics/statistical-review/bp-stats-review-2018-full-report.pdf. Accessed 07 Sept 2019
3. Ellabban O, Abu-Rub H, Blaabjerg F (2014) Renewable energy resources: current status, future prospects and their enabling technology. Renew Sust Energ Rev 39:748–764. https://doi.org/10.1016/j.rser.2014.07.113
4. Prasad Shadangi K, Mohanty K (2013) Characterization of nonconventional oil containing seeds towards the production of bio-fuel. J Renew Sustain Energy 5:033111. https://doi.org/10.1063/1.4808029
5. Mishra RK, Mohanty K (2018) Characterization of non-edible lignocellulosic biomass in terms of their candidacy towards alternative renewable fuels. Biomass Conv Bioref 8:799–812. https://doi.org/10.1007/s13399-018-0332-8
6. Singh YD, Mahanta P, Bora U (2017) Comprehensive characterization of lignocellulosic biomass through proximate, ultimate and compositional analysis for bioenergy production. Renew Energy 103:490–500. https://doi.org/10.1016/j.renene.2016.11.039
7. Doshi P, Srivastava G, Pathak G, Dikshit M (2014) Physicochemical and thermal characterization of nonedible oilseed residual waste as sustainable solid biofuel. Waste Manag 34:1836–1846. https://doi.org/10.1016/j.wasman.2013.12.018
8. Gupta M (2016) A review of pharmacological properties, pharmacognosy and therapeutic actions of Putranjiva roxburghii Wall. (Putranjiva). Int J Herb Med 4(6):104–108
9. Verma S (2016) Pharmacological review on cassia fistula linn (amaltas). Int J Pharm Chem Biol Sci 6(3):332–335
10. Verma SC, Vashishth E, Singh R, Kumari A, Meena AK, Pant P, Bhuyan GC, Padhi MM (2013) A review on parts of Albizia lebbeck (L.) Benth. Used as Ayurvedic drugs. Res J Pharm Tech 6(11):1307–1313
11. Naik S, Goud VV, Rout PK (2010) Characterization of Canadian biomass for alternative renewable biofuel. Renew Energy 35:1624–1631. https://doi.org/10.1016/j.renene.2009.08.033
12. Loo S Van, Koppejan J (2008) The handbook of biomass combustion & co-firing. Earthscan
13. Bhagwanrao SV, Singaravelu M (2014) Bulk density of biomass and particle density of their briquettes. Int J Agric Eng 7(1):221–224
14. Obernberger I, Thek G (2004) Physical characterisation and chemical composition of densified biomass fuels with regard to their combustion behaviour. Biomass Bioenergy 27:653–669. https://doi.org/10.1016/j.biombioe.2003.07.006
15. Basu P (2013) Biomass gasification, Pyrolysis and torrefaction: practical design and theory. https://doi.org/10.1016/C2011-0-07564-6
16. Mann BF, Chen H, Herndon EM (2015) Indexing permafrost soil organic matter degradation using high-resolution mass spectrometry. PLoS One 10:e0130557. https://doi.org/10.1371/journal.pone.0130557
17. Kim YM, Jeong J, Ryu S (2019) Catalytic pyrolysis of wood polymer composites over hierarchical mesoporous zeolites. Energy Convers Manag 195:727–737. https://doi.org/10.1016/j.enconman.2019.05.034
18. Wu Z, Wang S, Zhao J (2014) Synergistic effect on thermal behavior during co-pyrolysis of lignocellulosic biomass model components blend with bituminous coal. Bioresour Technol 169:220–228. https://doi.org/10.1016/j.biortech.2014.06.105
19. Broido A (1969) A simple, sensitive graphical method of treating thermogravimetric analysis data. J Polym Sci Part A-2 Polym Phys 7:1761–1773. https://doi.org/10.1002/pol.1969.160071012
20. Horowitz HH, Metzger G (1963) A new analysis of thermogravimetric traces. Anal Chem 35:1464–1468. https://doi.org/10.1021/ac60203a013
21. Mishra RK, Sahoo A, Mohanty K (2019) Pyrolysis kinetics and synergistic effect in co-pyrolysis of Samanea saman seeds and polyethylene terephthalate using thermogravimetric analyser. Bioresour Technol 289:121608. https://doi.org/10.1016/j.biortech.2019.121608
22. Pandey SP, Kumar S (2020) Valorization of argemone mexicana seeds to renewable fuels by thermochemical conversion process. J Environ Chem Eng 8:104271. https://doi.org/10.1016/j.jece.2020.104271
23. Fernandes ERK, Marangoni C, Souza O, Sellin N (2013) Thermochemical characterization of banana leaves as a potential energy source. Energy Convers Manag 75:603–608. https://doi.org/10.1016/j.enconman.2013.08.008
24. Nayan NK, Kumar S, Singh RK (2013) Production of the liquid fuel by thermal pyrolysis of neem seed. Fuel 103:437–443. https://doi.org/10.1016/j.fuel.2012.08.058
25. Demirbaş A (2005) Fuel and combustion properties of bio-wastes. Energy Sources 27:451–462. https://doi.org/10.1080/00908310490441863
26. Lynch MJ, Mulvaney MJ, Hodges HC, Thompson TL, Thomason WE (2016) Decomposition, nitrogen and carbon mineralization from food and cover crop residues in the central plateau of Haiti. SpringerPlus 5:973. https://doi.org/10.1186/s40064-016-2651-1
27. Mandal S, Pu S, Adhikari S, Ma H, Kim DH, Bai Y, Hou D (2020) Progress and future prospects in biochar composites: application and reflection in the soil environment. Crit Rev Environ Sci Technol. https://doi.org/10.1080/10643389.2020.1713030
28. Zhang H, Cheng YT, Vispute TP (2011) Catalytic conversion of biomass-derived feedstocks into olefins and aromatics with ZSM-5: the hydrogen to carbon effective ratio. Energy Environ Sci 4:2297. https://doi.org/10.1039/c1ee01230d
29. Seal S, Panda AK, Kumar S, Singh RK (2015) Production and characterization of bio oil from cotton seed. Environ Prog Sustain Energy 34(02):542–547. https://doi.org/10.1002/ep.12011
30. Wang Z, McDonald AG, Westerhof RJM (2013) Effect of cellulose crystallinity on the formation of a liquid intermediate and on product distribution during pyrolysis. J Anal Appl Pyrolysis 100:56–66. https://doi.org/10.1016/j.jaap.2012.11.017
31. Patwardhan PR, Satrio JA, Brown RC, Shanks BH (2010) Influence of inorganic salts on the primary pyrolysis products of cellulose. Bioresour Technol 101:4646–4655. https://doi.org/10.1016/j.biortech.2010.01.112
32. Duarte AT, Borges AR, Zmozinski AV (2016) Determination of lead in biomass and products of the pyrolysis process by direct solid or liquid sample analysis using HR-CS GF AAS. Talanta 146:166–174. https://doi.org/10.1016/j.talanta.2015.08.041
33. Han Z, Guo Z, Zhang Y (2018) Pyrolysis characteristics of biomass impregnated with cadmium, copper and jead: influence and distribution. Waste Biomass Valori 9:1223–1230. https://doi.org/10.1007/s12649-017-0036-5
34. Liu WJ, Tian K, Jiang H (2012) Selectively improving the bio-oil quality by catalytic fast pyrolysis of heavy-metal-polluted biomass:

take copper (Cu) as an example. Environ Sci Technol 46:7849–7856. https://doi.org/10.1021/es204681y

35. Carpenter AM (1998) Switching to cheaper coals for power generation. IEA Coal Research, London

36. Hupa M (2005) Interaction of fuels in co-firing in FBC. Fuel 84(10):1312–1319. https://doi.org/10.1016/j.fuel.2004.07.018

37. Armesto L, Bahillo A, Veijonen K (2002) Combustion behaviour of rice husk in a bubbling fluidised bed. Biomass Bioenergy 23:171–179. https://doi.org/10.1016/S0961-9534(02)00046-6

38. Wang G, Li W, Li B, Chen H (2008) TG study on pyrolysis of biomass and its three components under syngas. Fuel. 87:552–558. https://doi.org/10.1016/j.fuel.2007.02.032

39. Mohammed IY, Abakr YA, Kazi FK (2015) Comprehensive characterization of Napier grass as a feedstock for thermochemical conversion. Energies 8:3403–3417. https://doi.org/10.3390/en8053403

40. Sriram A, Swaminathan G (2018) Pyrolysis of Musa balbisiana flower petal using thermogravimetric studies. Bioresour Technol 265:236–246. https://doi.org/10.1016/j.biortech.2018.05.043